

Electrospraying the triblock copolymer SEBS: the effect of solvent system and the embedding of quantum dots

*Robin Koekoekx, Natalia C. Zawacka, Guy Van den Mooter, Zeger Hens, Christian Clasen**

R. Koekoekx, Prof. C. Clasen
Department of Chemical Engineering, Soft Matter, Rheology and Technology, KU Leuven,
3001 Leuven, Belgium
E-mail: christian.clasen@kuleuven.be

N. C. Zawacka, Prof. Z. Hens
Physics and Chemistry of Nanostructures, Center for Nano and Biophotonics, University of
Ghent, 9000 Ghent, Belgium

Prof. G. Van den Mooter
Department of Pharmaceutical and Pharmacological Sciences, Drug Delivery and Deposition,
KU Leuven, 3001 Leuven, Belgium)

Keywords: Block Copolymers, Colloids, Polymeric Materials, Quantum Dots,
Electrospraying

This work reports on ABA triblock copolymer microparticles encoded with CdSe/CdS core-shell quantum dots (QDs) realized by electrospraying. This method allows for simple but efficient embedding of QDs in polymer beads while retaining the fluorescent properties of the original QDs. The creation of poly(styrene-ethylene-butylene-styrene) (SEBS) monodisperse spherical microparticles with a tunable morphology for applications of the final QD loaded product is attainable via solvent variation. By varying the selectivity of the solvent for one of the distinct blocks in the polymer, the final particle morphology can be selectively altered while maintaining the same overall process conditions, allowing to tailor the particles from homogeneously flat in a non-selective solvent to dense spherical particles in an endblock selective solvent system. The mechanism responsible for this transition in morphology could be related to differences in mass transfer in the droplets and thus solvent evaporation rates arising from particular microphase structures. Finally, fluorescence characteristics of the final QD embedded polymer particles and photodegradation stability are investigated by spectrophotometry and are compared to the temporal evolution of the original quantum dots,

indicating significant stability improvement and well dispersed QDs in an optimized polymer matrix morphology.

1. Introduction

Semiconductor nanocrystals or quantum dots (QDs) gained large research interest over the last decade due to their exceptional electronic and optical properties, such as high brightness, broad absorption spectra, very narrow but tunable emission spectra, and strong resistance to photobleaching.^[1] The size, shape and material of the QDs, which are adjustable during synthesis, determine their final fluorescent emission properties. These inorganic nanomaterials have seen a dramatic rise in functionality and effectiveness due to recent technological findings in their synthesis process, the creation of core-shell QDs and the ability to functionalize the nanocrystals for certain applications.^[2] These inorganic semiconductor nanoparticles show great potential as replacement for common organic dyes since they can be utilized for multiplex analysis and long-term studies.^[1a,3] Furthermore, QDs are investigated for a multitude of other applications including photovoltaics^[4], photodetection^[5] and lighting in LEDs and displays.^[6] However, due to the nature of their building blocks, QDs generally exhibit undesirable properties like cytotoxicity, low stability in an oxygen-rich environment and poor biocompatibility, in particular for *in-vivo* and *in-vitro* imaging, which limits their current applicability. To increase the relevance of these materials in diagnostics and photodetection, one possible route is to alter or coat the quantum dot surface to improve on the aforementioned negative properties and to provide application suited surface functionalities.

Two possible approaches utilizing polymers as protective coatings are reported: coating each QD individually^[3,7], or embedding multiple QDs into a single polymer matrix.^[8] In this paper, we explore the latter option, utilizing electrospraying as a suitable means to produce the polymer matrix in form of monodisperse micro- and nanoparticles. Embedding QDs in

polymeric fibers by electrospinning^[9] or other techniques^[10] is another often explored route with a multitude of possible applications, however, in this paper the focus is on the production of QD loaded electrosprayed polymer particles, as this allows to exploit their colloidal properties that are beneficial for mechanical handling, dispersability in media and adsorption behavior, as well as their dry powder flowability.^[7] Other methods that have been investigated to embed polymer beads with QDs, include microfluidic jet-mode breakup^[11], suspension polymerization^[12] and the swelling method^[13] among others.^[14]

Electrospray or electrohydrodynamic atomization is an efficient technique to generate narrow size distributed micro- or nanoparticles with tailored size, morphology and microstructure (**Figure 1**). By applying a high electric potential difference between a nozzle and a collector, surface charges are added to a liquid pumped through the nozzle at a constant flowrate. Due to the induced electric stress, the liquid forms a Taylor-cone, out of which a jet protrudes, which will eventually break up into small droplets due to capillarity. The emitted charged droplets are attracted towards the grounded collector, while rapid evaporation is occurring for liquids of sufficiently low boiling point. If all of the liquid is able to evaporate during the droplet trajectory, dry particles of any remaining solute are gathered on the collector. In case of a polymer as a solute, electrospinning of polymer fibers can occur if the polymer concentration is increased above a critical limit, so that the elastic properties of the polymer solution are sufficient to stabilize the jet, preventing capillary breakup.^[15] Currently, electrospraying of polymers finds a multitude of applications in various fields, for example in the pharmaceutical industry, to create complex drug delivery systems, where active pharmaceutical ingredients (APIs) are added to single particles or as core-shell configurations if a coaxial nozzle is employed.^[16]

With this technique, QD embedded particles can be created in a single step with a relatively easy setup under controlled atmospheric conditions. The size of the particles can be tuned from

~ 100 nm - 10 μ m and a wide variety of polymers can be electrosprayed. Furthermore, due to the rapid solvent evaporation in the small droplets, the QDs are expected to remain well dispersed in the polymer since the period of time in which they can freely move and aggregate is very limited.^[9a] This minimization of clustering and thus interaction between the QDs ensures that the quantum yield of the QDs remains high.^[12a,17] Different research groups have shown that Förster energy transfer (FRET) can be effectively eliminated in electrospun fibers, preserving the original fluorescent properties of the QDs.^[9] Even though electrospraying is a very attractive technique in the context of QD embedded microparticle generation, very little literature exists on this subject. Sun et al. have reported the production of electrosprayed poly(styrene-acrylate) microspheres containing CdSe/ZnS nanocrystals for biomolecule detection, but little investigation in the final fluorescence performance of the particles was conducted.^[8b] As mentioned before, multiple groups have reported on the preparation of electrospun polymeric fibers containing QDs^[9] or on the production of electrosprayed QD embedded polymeric thin films^[18], however there is a clear absence of published research in the production of QD encoded beads, specifically by electrospraying, and the effect that the process has on the final performance of the product.

In the current paper, we investigate the possibility to embed CdSe/CdS quantum dots in block copolymer particles using electrospraying. The polymer of interest is a linear triblock ABA-type copolymer polystyrene-b-poly(ethylene-butylene)-b-polystyrene (SEBS) that has previously been utilized to embed the same type of QDs in a bulk polymer matrix.^[19] The midblock of this commercially available amorphous thermoplastic elastomer has shown favorable interaction with the CdSe/CdS QDs, resulting in a reduction of aggregation and improved stability compared to other similar polymers.^[20] In addition to this stabilizing effect of the ABA copolymer on the quantum dots, a block copolymer has been chosen as it will also allow to vary the configuration of the polymer chain and its structure in solution, depending on

the interaction potential of the monomeric constituents within different selected solvents. Linear ABA block copolymers exhibit spontaneous microphase separation due to the dissimilarity in the chemical structure of their distinct blocks.^[21] Considering the difference in solubility parameters, solvents can be either selective for a certain block or non-selective for the complete polymer. Minimizing the enthalpic energy by reducing the contact between a specific block and a selected non-solvent drives the system into different microphase structures.^[21,22] In particular the possibility to gradually transition between non-crosslinked core-corona micellar structures to networks created by aggregated endblock domains will be utilized in the current paper to study effects of the solvent-dependent microphase structure in ABA block-copolymer solution on the electrosprayability and resulting particle morphology.^[22,23] Finally, the core-shell QDs are embedded in the polymer particles with the preferred morphology for applications and are characterized with respect to their quantum efficiency and stability evolution in comparison to the initial QDs in suspension.

2. Results and discussion

2.1. Electrospraying SEBS polymer particles

The final morphology of electrosprayed polymer microparticles depends to a large extent on the initial polymer concentration.^[16b,24] Porous, wrinkled or buckled particles are more likely to be generated at low polymer concentration, while more dense, spherical particles can be generated by electrospraying at higher polymer concentration. For the embedding of QDs in this paper, spherical monodisperse polymer particles should be created to assure the production of a homogenous product containing evenly dispersed QDs with uniform stability and fluorescent properties. Thus, the concentration of the polymer in the solution was aimed to be maximized, while maintaining electrosprayability into droplets without the production of any fibers. Palangetic et al. have shown that the minimum polymer concentration to create fibers is related to the elastic properties of the polymer in solution by proposing an extensibility average

molecular weight M_L , relevant for highly extension dominated processes.^[15a] They suggest that the classical power law scaling $c_{spin} \sim M^{-(1-3\nu)}$ which can be used to approximate the highest concentration that can be electrospayed from a solvent of a given quality and an excluded volume exponent ν without creating fibers, is only applicable for sufficiently low polymer molecular weights. GPC measurements show that the weight average molecular weight M_w of the SEBS is 8.1×10^4 g/mol with a polydispersity index (PDI) of 1.08 (**Table 1**). A comparison to the molecular weights limits given in Palangetic et al., beyond which the high molecular weight stabilization and scaling laws are valid and which is on the order of $O(10^5$ g/mol) for polymers in athermal and good solvents, indicates that the current SEBS polymer falls into the low molecular weight scaling regime. In this regime, an earlier assumption, that the upper concentration limit for particle formation by electrospaying is proportional to the entanglement concentration c_{ent} , is still valid.^[25] For such lower molecular weights in the semi-dilute entangled regime, the polymer chains form a sufficient number of polymer entanglements such that the extensional viscosity and relaxation time of the solution are high enough to resist disturbances in the jet, preventing capillary breakup into small droplets and promoting the formation of polymer fibers. Based on arguments introduced by Gupta et al., a combination of fiber and bead formation is possible, depending on the molecular weight of the polymer, already when the overlap concentration c^* is reached (entering the semi-dilute unentangled regime).^[26]

However, in the case of ABA block copolymers, the polymer can self-assemble into different microphase structures with different viscoelastic properties depending on which solvent system is present, so that the conventional scaling criteria based on a single overlap or entanglement concentration are likely not sufficient^[27]. Specifically, the polymer of interest, SEBS, forms a self-assembly depending on the solvent system's selectivity for either PS (endblock) or PEB (midblock).^[22,23,28] A schematic illustration for the two extreme cases where the solvent system is selective for one of the distinct blocks, is shown in **Figure 2**. If the solvent system is

preferentially solvating the PEB midblock, the PS endblocks aggregate, forming micellar PS-zones (Figure 2a). The conformation of the midblock can include dangling ends, loops where both PS blocks end in the same domain or links from one PS zone to another, thus forming bridges between these endblock micelles, creating a linked network.^[28b] The network conformation most abundantly present in a certain system depends mainly on midblock fraction, solvent properties and concentration.^[22,23b] On the other hand, a solvent system which is selective for the PS endblock will result in an independent core-corona micellar structure due to the aggregation of the midblock PEB into discrete domains to minimize contact with the solvent (Figure 2b).^[22] In this case, the PS chains will preferentially be present in its selective solvent, forming a non-crosslinked corona.^[23] The presence of midblock bridges in the first case, resulting in a crosslinked network with gel-like properties, leads to a dramatically higher elasticity of the system than in the non-crosslinked micellar case, which will additionally influence the electrosprayability of the solution.^[28a,29] This is supported by observations of Wang et al., who have shown for SEBS that the final electrosprayed/spun product morphology greatly depends on the present microphase structure when investigating the fiber-to-bead transition in different solvent systems.^[23b]

Hansen solubility parameters, often utilized in solvent selection for electrospraying/spinning processes, give insight in the solvent quality for the different blocks of the block copolymer, allowing for microphase structure prediction^[30]. The generally well electrosprayable solvents CHCl_3 and DCM used in the current investigation represent good solvents for both the PS and the PEB blocks according to its Hansen solubility parameters (**Table 2**) (relative energy difference $\text{RED} < 1$).^[31] The resulting molecular conformation leans more to the case of a selective solvent for the midblock (Figure 2a) due to the incompatibility of PS and PEB and the relatively large mid- to endblock ratio, promoting a separation into PS zones.^[23a,28a] By adding an adequate amount of PEB non-solvent DMF to the originally non-selective solvent, the

complete solvent system will become a non-solvent for the midblock ($RED \geq 1$). The maximum fraction of the non-solvent DMF that can be added to still dissolve the polymer according to Hansen solubility factors equates to 35% by volume and 20% by volume for $CHCl_3$ and DCM respectively. Hence, the microphase structure changes to a micellar structure without interconnection (Figure 2b). The possibility of such a structural shift between a good solvent for both blocks and a selective solvent for the endblock was also shown by Wang et al. by utilizing small angle X-ray scattering (SAXS).^[23b]

When determining the maximum concentration to electro spray solely particles, it suffices to investigate the concentration regimes for the system that intrinsically will exhibit stronger elongational properties already at lower concentrations, in this case for a single solvent system (molecular structure similar to Figure 2a). The maximal polymer concentration found for this solvent system will also be used for the dual solvent system to demonstrate the effect of solvents on final particle morphology.

To assure that no polymer chain interaction occurs in the original solution, the overlap concentration c^* correlated to the theoretical maximum electro sprayable concentration is determined from the kinematic viscosity measured with an Ubbelohde setup. Firstly, the specific viscosity η_{sp} is determined for a wide range of concentrations for SEBS in $CHCl_3$, as shown in **Figure 3**. The limits of the different concentration regimes of interest can be found by identifying the intersections of the different power law scaling fits with distinct exponents. In this way, $c_{CHCl_3}^* = 12.2$ mg/ml, $c_{ent,CHCl_3} = 49.1$ mg/ml is found. Alternatively, c^* can be evaluated using the expression $c_a^* = 0.77/[\eta]$, where the intrinsic viscosity $[\eta]$ is determined by fitting the reduced viscosity η_{red} to zero concentration (**Figure 4**).^[32] This method equates to a similar result for the $CHCl_3$ solution, $c_{a,CHCl_3}^* = 11.5$ mg/ml and gives $c_{a,DCM}^* = 19.6$ mg/m for the DCM solution. Based on these results, a concentration of 10 mg/ml in the dilute regime was

chosen to create the SEBS particles by electrospraying for all solvent systems to avoid any fiber formation.

Subsequently, polymer solutions containing 10 mg/ml of SEBS in the different single or dual solvent system indicated in Table 2 were electrosprayed under exactly the same process and environmental conditions. SEM imaging was then utilized to investigate different morphologies of the final polymer particles, which in turn is correlated to the molecular conformation of the polymer present during solvent evaporation. The results of the SEM imaging of all the different particle morphologies are shown in **Figure 5**. Generally it is observed that, when the polymer is electrosprayed from either non-selective solvent, flat “pancake”-like structures are obtained on the collector (Figure 5a and 5b). In contrast to this, particles created from an endblock selective solvent polymer solution are more spherical and monodisperse (Figure 5d and 5e).

The proposed mechanism for this phenomenon is the following. When the jet of polymer solution breaks up into small charged droplets, rapid solvent evaporation occurs due to the large surface to volume ratio. A higher concentration at the surface arises, resulting in a concentration gradient inside the droplet.^[24] The time scale of evaporation $\tau_{ev} = l/v_{ev}$ in this process is much smaller compared to the timescale of polymer chain diffusion $\tau_D = l^2/D$, so this concentration gradient persists over the lifetime of the droplet, which will result in initially high Peclet numbers $Pe = \tau_D/\tau_{ev} = v_{ev} l/D$, where v_{ev} is the evaporation rate, l is a characteristic length and D is the diffusion coefficient.^[33] The form of this concentration gradient and the evolution thereof depends then on the solvent/polymer interaction as well as the concentration of the polymer:

In case of a non-selective solvent, solvent evaporation will occur initially fast. However, the crosslinked molecular conformation of the polymer at higher concentrations will result in skin formation at the surface of the droplet when its gel concentration ϕ_N is reached, resulting in a

strong concentration gradient localized close to the surface, as proven in numerical calculations by Doi et al.^[34] This gel layer will act as a barrier, drastically hindering solvent transport to the surface from the inside of the droplet and significantly lowering the solvent evaporation rate v_{ev} , as indicated in the schematic in Figure 5c.^[35] Hence, not all solvent can evaporate from the droplets during their trajectory towards the collector. Due to the elastic properties of the gel-like skin, the droplet will still be able to deform when impacting onto the collector. The strength of the skin layer will then determine the degree spreading over the collector, and in how far the liquid core will be exposed upon impact droplets and how freely the remaining solvent can evaporate from the surface. In case of CHCl_3 as the solvent, large flat polymer particles are created, which remain intact, so that the single particles can still be identified (Figure 5a). Using DCM as the solvent results in similar particles but they appear to be less stable and show a very rough structure (Figure 5b). This is expected to occur due to rapid solvent evaporation after spreading on the collector because of the lower boiling point of DCM ($T_b = 39.6 \text{ }^\circ\text{C}$) compared to CHCl_3 ($T_b = 64.2 \text{ }^\circ\text{C}$) and the lower polymer loading of the initial polymer solution ($c_{DCM}/c_{a,DCM}^* = 0.51$ while $c_{\text{CHCl}_3}/c_{a,\text{CHCl}_3}^* = 0.87$).

In the case of the PS selective dual solvent system, the solvent evaporation is less hindered by the non-crosslinked microstructure, resulting in a more uniform concentration gradient over the whole particle as indicated in Figure 5d. The polymer concentration needed to form a gel-like structure at the surface in this micellar case (ϕ_S) is much higher compared to the other case ($\phi_S \gg \phi_N$), resulting in the absence of a strong gel-like skin layer during the lifetime of the droplet.^[34] This absence of a localized high gradient and no skin formation allows the solvent to evaporate from the droplets while they are falling towards the collector. This results in spherical monodisperse SEBS particles as observed in Figure 6a for CHCl_3/DMF 65/35 v/v and Figure 5e for DCM/DMF 80/20 v/v.

If one would simply investigate the difference in evaporation rates v_{ev} (or boiling points) of the two solvent systems containing CHCl_3 for example without taking into account the polymer structure during droplet trajectory, different conclusions would be made. Experimentally determined evaporation rates show that the system of CHCl_3/DMF has an evaporation rate less than half that of CHCl_3 ($v_{ev,\text{CHCl}_3/\text{DMF } 65/35} = 0.447 \text{ g/m}^2\text{s}$ and $v_{ev,\text{CHCl}_3} = 1.14 \text{ g/m}^2\text{s}$). So, one could assume that for the same electro spraying conditions, it is more likely that more solvent would still be present in the CHCl_3/DMF system. The opposite is true, all of the solvent has evaporated and spherical particles are created in that case, while for the CHCl_3 system flat, deformed particles are produced.

2.2. Quantum dot embedded SEBS particles

The absorption and emission spectra of the neat hydrophobic QDs in CHCl_3 are represented in **Figure 6**. When excited with a laser at 450 nm, the QDs emit light with a peakwavelength at 627 nm, a full width at half maximum (fwhm) of 37.4 nm and exhibit a photoluminescence quantum yield (PLQY) of 62.6%. They mainly absorb light at lower wavelengths, below 500 nm. To embed the CdSe/CdS core-shell QDs in the polymer particles, the QDs are simply added to the polymer solution producing the monodisperse, more spherical particles, namely the CHCl_3/DMF 65/35 v/v solution. The addition of the QDs to this system is not expected to alter any of the solution properties, thus producing exactly the same particle morphologies as in **Figure 5d**. Hence, the electro spraying method results in a one-step production of QD embedded particles without time consuming preparation or additional post-process washing steps.

The normalized fluorescence spectra of the neat QDs in solvent and the QD embedded SEBS particles are compared in **Figure 7**. The spectra are very similar without any evidence of peak shape distortion: the fwhm stays the same while the peakwavelength shifted to 629 nm. This small redshift (2 nm) indicates that the QDs are well dispersed and separated in the polymer

particles, since a larger shift of the peakwavelength is normally found when QDs are allowed to aggregate and interact with each other.^[19,36] The current difference in peakwavelength of 2 nm is very limited compared to products from slower processes like film casting for example, where extensive QD aggregation can occur.^[9a,19,36] The PLQY dropped from 62.6% to 48.8 % when the QDs were added to the particles. This phenomenon has been observed before and can be related to self-absorption and/or ligand loss of the QDs.^[19,37] Ligand loss should be limited for this polymer/QD combination, since the polymer's alkyl chains are very similar in chemical composition to the oleic acid ligands on the core-shell QDs.^[20] The decrease in PLQY is most likely due to self-absorption, where QDs in the particles absorb the emitted light from other QDs in the vicinity.^[19] Furthermore, electro spraying allows for efficient embedding of QDs in the SEBS particles, since the dispersing medium of encoded beads shows no fluorescent behavior resulting from free uncoated QDs that get extracted from the particles.

Finally, a photodegradation stress test has been performed to compare the photostability of the neat QDs and the QD encoded particles in an open environment (**Figure 8**). After 60 min, a decrease of fluorescence intensity of ~20% was found for the neat QDs in CHCl₃, while the embedded particles only lost ~10% of initial intensity. A difference in degradation rate can also be noted for the two samples, a 2nd order intensity decrease for the neat QDs in solvent while the decrease in intensity for the encoded particles follows a linear trend, indicating that the embedding in SEBS indeed has a significant influence on the stability of the QDs.

The solvent tunable electro spraying process shows a lot of promise to generate application specific particle shapes containing QDs, due to its simple but efficient principle to transfer the QDs well dispersed into polymer beads. A wide range of block copolymers in different ratios of solvent mixture can be utilized to this end, since the generally rapid evaporation rates present in this process will more easily lead to non-aggregated QDs compared to techniques operating

at longer timescales. It was furthermore shown by Sun et al. that increasing the fluorescence intensity of the final encoded beads is easily achieved by increasing the QD concentration in the original polymer solution.^[8b] Moreover, multicolor encoding of beads is trivial by adding different QD species emitting light at different wavelengths in the polymer solution to be electrosprayed.^[8b] This research makes us believe that the electrospraying technique can serve as a powerful technique to produce functional QD-embedded microparticles for a wide variety of applications.

3. Conclusion

The electrospraying technique is successful in embedding QDs in ABA triblock copolymer particles in an efficient but simple one-step process, while retaining the original QD fluorescent properties. In electrospraying, the employed solvent system is of primary importance for the morphology of the final polymer microparticles, especially for ABA triblock copolymers. Depending on whether a good solvent for both blocks or a selective solvent for the endblock is utilized for the electrosprayable polymer solution, completely different particle morphologies can be produced under exactly the same process conditions and polymer concentration. We could correlate this to the distinct change in the underlying microphase structure that the block copolymer SEBS exhibits in different solvent systems, and the resulting modification of the mass transfer that occurs during the droplet trajectory towards the collector. Specifically, we backed the hypothesis that a solution of SEBS in non-selective solvent CHCl_3 produces flat pancake-like particles due to the strong skin formation at the surface of the droplet during their fall towards the collector, which reduces the solvent evaporation rate drastically. In the end, solvent is still present in the droplets when they impact onto the collector, causing the droplets to spread open due to its elastic gel-like properties, after which the remaining solvent can freely evaporate. On the other hand, when a solvent system of CHCl_3 and DMF is used which is a non-solvent for the midblock PEB, more spherical monodisperse particles are formed due to

the absence of strong skin formation and complete solvent evaporation during flight, resulting from the core-corona micelle structure present in this system. CdSe/CdS QDs were successfully embedded into the optimized SEBS polymer microparticles by electrospraying the latter polymer solution. By investigating the emission spectra of the products with the original QDs in solvent, it is shown that the QDs remain well dispersed in the final particles due to the very limited redshift of 2 nm, which is in general much more significant when aggregation does occur. Photodegradation stress tests prove that the stability of the QDs is improved compared to their initial state: 10% more of the initial intensity was retained compared to the neat QDs after 60 min and the degradation behavior is altered to a 1st order decrease from a 2nd order one.

4. Experimental Section

Materials

The linear triblock copolymer polystyrene-*b*-poly(ethylene-butylene)-*b*-polystyrene (SEBS) with a polystyrene (PS) fraction of 30 wt% and a maleic anhydride content of 1.4 - 2 wt% grafted onto the midblock (commercially available as Kraton FG1901 G) was obtained from Kraton (Houston, USA). Chloroform (CHCl₃) (99.2 %) was purchased from VWR Chemicals (Leuven, Belgium), dichloromethane (DCM) (>99 %) from Fisher Scientific (Loughborough, UK), N,N-dimethylformamide (DMF) (99.8 %) and tetrahydrofuran (THF) (>99 %) from Acros Organics (Geel, Belgium).

For the production of the CdSe/CdS core-shell particles, the following materials were used. CdO (≥99.99%), and oleyl alcohol (OLOH) (85%) were obtained from Sigma-Aldrich (St-Louis, USA). N-tetradecylphosphonic acid (TDPA) (≥97%) was purchased from PlasmaChem GmbH (Berlin, Germany). Trioctylphosphine (TOP) (≥97%) and sulfur (99.999%) were purchased from Strem Chemicals (Newburyport, USA). Trioctylphosphine oxide (TOPO) was purchased from Merck Millipore (Darmstadt, Germany). Selenium (200 mesh, 99.999%) and oleic acid (90%) were obtained from Alfa Aesar (Ward Hill, USA). The reaction solutions of TOP-Se (2

M) and TOP-S (2.4 M) were prepared by dissolving 1.56 g of the Se powder and 0.77 g of sulfur in 10 mL of TOP respectively.

CdSe/CdS core-shell QDs were synthesized by adapting the previously reported procedures^[38], where the wurtzite CdSe cores are synthesized separately and the CdS shell is grown around them. CdSe wurtzite particles were produced starting from CdO, TDPA, OIOH and 10 g of TOPO, molar ratio Cd:TDPA:OIOH 1:6:16. The reaction mixture was kept for 1h at 150 °C under nitrogen atmosphere. The solution was then heated to 350 °C in order to dissolve CdO, then 2 mL of TOP was injected, followed by the injection of 2 M TOP-Se solution, Cd:Se molar ratio 1:2. The reaction time is limited to a few seconds and stopped by a drop in temperature. The QDs were then precipitated from 20 ml of methanol and collected by centrifugation at 4000 rpm for 3 min. The supernatant was discarded and the QDs were purified with toluene and methanol.

CdSe/CdS wurtzite particles were synthesized from CdO, oleic acid and 5 g of TOPO; Cd:oleic acid molar ratio 1:5. The reaction mixture was heated for 1h at 150 °C under nitrogen atmosphere. The solution was then heated to 350 °C in order to dissolve CdO, then 1 mL of TOP was injected, followed by the injection of 2 ml of reaction solution. The reaction solution consisted of previously synthesized QD seeds of CdSe, 2.4 M TOP-S solution and additional TOP solvent; Cd:S molar ratio 1:1.2. After 5 minutes, the reaction was quenched by a drop in temperature and the particles precipitated with 10 ml of methanol. The QDs were collected by centrifugation at 4000 rpm for 3 min and purified twice with toluene and methanol. The QDs were dispersed and stored in toluene.

Polymer solutions were prepared by dissolving the necessary amount of SEBS in either pure CHCl₃, DCM or a mixture of CHCl₃/DMF (up to 65/35 v/v), or DCM/DMF (up to 80/20 v/v) at room temperature (25°C) for 24 hours with continuous stirring to obtain a polymer concentration of 10 mg/ml. CdSe/CdS QDs were added to the SEBS in CHCl₃/DMF in a concentration of 0.06 μmol QDs/mg polymer.

Polymer solution characterization

Kinematic viscosities of different concentrations of SEBS in chloroform have been determined with an Ubbelohde viscometer (Schott AG, Mainz, Germany), using capillaries 0a and 1c (SI Analytics, Mainz, Germany), depending on the kinematic viscosity of the sample to obtain measurement times in the proposed range. Measurements for each sample were repeated three times.

The molecular weight distribution of the SEBS sample has been determined with gel permeation chromatography (GPC) measurements using a Shimadzu GPC LC-20 (Shimadzu, Tokyo, Japan) with a PLgel 5 μm MIXED-D column (300 x 7,5 mm) in THF. The sample contained 1 mg/ml of SEBS in THF and was first filtered with a disposable Teflon filter (Machery-Nagel, Düren, Germany) with a pore size of 0.2 μm . The measurement was performed at 35°C at a flowrate of 1 ml/min.

Evaporation rates of the polymer solutions were determined in a climate controlled environment at 30°C and 20% relative humidity. For this, an amount of polymer solution between 2-4 mg was added to a glass petridish of 0.056 m diameter. The weight of the solution was monitored on a weighing balance Sartorius CPA225D (Sartorius Weighting Technology, Goettingen, Germany) over regular time intervals of 10 s during at least 5 min.

Electrospraying

Electrospraying was performed in a climate controlled electrospinning apparatus (EC-CLI, IME Technologies, Geldrop, The Netherlands) at 30 °C and 20% relative humidity. The polymer solution was expelled from a syringe through a nozzle of inner diameter $D = 0.51$ mm (21 gauge) at a constant flowrate of 0.5 ml/h by a syringe pump (Harvard Apparatus, Holliston, MA, USA). For all produced particles, a potential difference of 23-25 kV between the needle

and a grounded collector was applied to generate stable cone-jet operation, with a fixed needle tip-to-collector distance of 18 cm.

Particle morphology

The particle morphology was imaged with scanning electron microscopy (SEM). The particle samples were directly electrosprayed onto aluminum foil and platinum coated with a SCD-030 Balzers Union sputter-coater (Oerlikon Balzers, Balzers, Liechtenstein). A Phillips XL30 SEM-FEG (Philips, Eindhoven, The Netherlands) equipped with a Schottky field emission electron gun and a conventional EverhartThornley secondary electron detector was used to record images with an acceleration voltage of 20 kV and a spot size at 3.

Neat QDs and QD-embedded polymer particles characterization

Bright field transmission electron microscopy (TEM) images were taken using a Cs corrected JEOL 2200 FS microscope (JEOL USA, Inc., Peabody, USA). Absorption spectra were obtained using PerkinElmer Lambda 950 spectrometer (PerkinElmer, Waltham, USA).

The concentration of the wurtzite QDs dispersion was determined by their absorbance and the intrinsic absorption coefficients based on the Maxwell–Garnett effective medium theory.^[1b,39]

The size of the CdSe was determined from the position of the first excitonic absorption peak using the sizing curve of Mulvaney et al., resulting in 3.12 nm particles. The size of the complete QDs was determined by TEM analysis, obtaining a diameter of 8.1 nm (+/- 1.1 nm) for the CdSe/CdS QDs (see **Figure 9**).^[40]

The emission spectra of both the original QDs in solvent and the QD embedded polymer particles were determined on a FLSP920 UV-Vis-NIR spectrofluorometer (Edinburgh instruments LTD, Livingston, UK). The ratio of emitted number of photons to the absorbed number of photons or photoluminescence quantum yield (PLQY) was determined by an integrating sphere analysis via the two-measurement approach, resulting in an efficiency of

62%.^[41] An inverted laser scanning confocal microscope Leica TCS SP8 (Leica, Mannheim, Germany) was utilized to perform the photodegradation test using a 20 mW laser of 488 nm at an intensity of 50% during 60 min.

Acknowledgements

Financial support from the Fonds Wetenschappelijk Onderzoek – Vlaanderen (FWO, grant no. G0A3916N) and the Vlaanderen Agentschap Innoveren & Ondernemen (VLAIO, SIM SBO-project QDOCCO) is acknowledged.

Received: ((will be filled in by the editorial staff))

Revised: ((will be filled in by the editorial staff))

Published online: ((will be filled in by the editorial staff))

References

- [1] a) I. L. Medintz, H. T. Uyeda, E. R. Goldman, H. Mattoussi, *Nat. Mater.* **2005**, *4*, 435; b) Z. Hens, I. Moreels, *J. Mater. Chem.* **2012**, *22*, 10406; c) R. Gill, M. Zayats, I. Willner, *Angew. Chemie Int. Ed.* **2008**, *47*, 7602; d) I. Moreels, Y. Justo, B. De Geyter, K. Haestraete, J. C. Martins, Z. Hens, *ACS Nano* **2011**, *5*, 2004; e) T. Jamieson, R. Bakhshi, D. Petrova, R. Pocock, M. Imani, A. M. Seifalian, *Biomaterials* **2007**, *28*, 4717.
- [2] T. M. Jovin, *Nat. Biotechnol.* **2003**, *21*, 32.
- [3] A. F. E. Hezinger, J. Teßmar, *Eur. J. Pharm. Biopharm.* **2008**, *68*, 138.
- [4] a) J. Tang, K. W. Kemp, S. Hoogland, K. S. Jeong, H. Liu, L. Levina, M. Furukawa, X. Wang, R. Debnath, D. Cha, K. W. Chou, A. Fischer, A. Amassian, J. B. Asbury, E. H. Sargent, *Nat. Mater.* **2011**, *10*, 765; b) J. M. Luther, M. Law, M. C. Beard, Q. Song, M. O. Reese, R. J. Ellingson, A. J. Nozik, *Nano Lett.* **2008**, *8*, 3488.
- [5] a) T. Rauch, M. Böberl, S. F. Tedde, J. Fürst, M. V. Kovalenko, G. Hesser, U. Lemmer, W. Heiss, O. Hayden, *Nat. Photonics* **2009**, *3*, 332; b) G. Konstantatos, E. H. Sargent, *Nat. Nanotechnol.* **2010**, *5*, 391.
- [6] a) T.-H. Kim, K.-S. Cho, E. K. Lee, S. J. Lee, J. Chae, J. W. Kim, D. H. Kim, J.-Y. Kwon, G. Amaratunga, S. Y. Lee, B. L. Choi, Y. Kuk, J. M. Kim, K. Kim, *Nat. Photonics* **2011**, *5*, 176; b) S. Abe, J. J. Joos, L. I. Martin, Z. Hens, P. F. Smet, *Light Sci. Appl.* **2017**, *6*, e16271; c) E. Jang, S. Jun, H. Jang, J. Lim, B. Kim, Y. Kim, *Adv. Mater.* **2010**, *22*, 3076.
- [7] Y. Gao, S. Reischmann, J. Huber, T. Hanke, R. Bratschitsch, A. Leitenstorfer, S. Mecking, *Colloid Polym. Sci.* **2008**, *286*, 1329.
- [8] a) N. Tomczak, D. Jańczewski, M. Han, G. J. Vancso, *Prog. Polym. Sci.* **2009**, *34*, 393; b) L. Sun, X. Yu, M. Sun, H. Wang, S. Xu, J. D. Dixon, Y. A. Wang, Y. Li, Q. Yang,

- X. Xu, *J. Colloid Interface Sci.* **2011**, 358, 73; c) W. B. Tan, Y. Zhang, *Adv. Mater.* **2005**, 17, 2375; d) W. Chen, J. Lei, Y. Wang, P. M. Mendes, Z. Zhang, Q. Hu, Y. Xiong, J. Pan, *Macromol. Mater. Eng.* **2019**, 304, 1.
- [9] a) M. Li, J. Zhang, H. Zhang, Y. Liu, C. Wang, X. Xu, Y. Tang, B. Yang, *Adv. Funct. Mater.* **2007**, 17, 3650; b) X. He, L. Tan, X. Wu, C. Yan, D. Chen, X. Meng, F. Tang, *J. Mater. Chem.* **2012**, 22, 18471; c) S. Schlecht, S. Tan, M. Yosef, R. Dersch, J. H. Wendorff, Z. Jia, A. Schaper, *Chem. Mater.* **2005**, 17, 809; d) J. S. Atchison, C. L. Schauer, *Sensors* **2011**, 11, 10372; e) E. T. Hwang, R. Tatavarty, H. Lee, J. Kim, M. B. Gu, *J. Mater. Chem.* **2011**, 21, 5215.
- [10] a) C. Meng, Y. Xiao, P. Wang, L. Zhang, Y. Liu, L. Tong, *Adv. Mater.* **2011**, 23, 3770; b) S. Yang, C. F. Wang, S. Chen, *J. Am. Chem. Soc.* **2011**, 133, 8412; c) P. L. Heseltine, J. Ahmed, M. Edirisinghe, *Macromol. Mater. Eng.* **2018**, 303, 1800218.
- [11] S.-K. Lee, J. Baek, K. F. Jensen, *Langmuir* **2014**, 30, 2216.
- [12] a) S. V Vaidya, A. Couzis, C. Maldarelli, *Langmuir* **2015**, 31, 3167; b) P. O'Brien, S. S. Cummins, D. Darcy, A. Dearden, O. Masala, N. L. Pickett, S. Ryley, A. J. Sutherland, *Chem. Commun.* **2003**, 3, 2532.
- [13] a) Y. Wei, X. Deng, Z. Xie, X. Cai, S. Liang, P. Ma, Z. Hou, Z. Cheng, J. Lin, *Adv. Funct. Mater.* **2017**, 27, 1703535; b) M. Bradley, N. Bruno, B. Vincent, *Langmuir* **2005**, 21, 2750.
- [14] W. Sheng, S. Kim, J. Lee, S. W. Kim, K. Jensen, M. G. Bawendi, *Langmuir* **2006**, 22, 3782.
- [15] a) L. Palangetic, N. K. Reddy, S. Srinivasan, R. E. Cohen, G. H. McKinley, C. Clasen, *Polymer* **2014**, 55, 4920; b) J. H. Yu, S. V. Fridrikh, G. C. Rutledge, *Polymer* **2006**, 47, 4789.
- [16] a) D. N. Nguyen, C. Clasen, G. Van den Mooter, *Eur. J. Pharm. Biopharm.* **2017**, 113, 50; b) N. Bock, M. A. Woodruff, D. W. Hutmacher, T. R. Dargaville, *Polymers* **2011**,

- 3, 131; c) M. Enayati, M. W. Chang, F. Bragman, M. Edirisinghe, E. Stride, *Colloids Surfaces A Physicochem. Eng. Asp.* **2011**, 382, 154.
- [17] a) C. R. Kagan, C. B. Murray, M. G. Bawendi, *Phys. Rev. B* **1996**, 54, 8633; b) J. Lee, A. O. Govorov, N. A. Kotov, *Nano Lett.* **2005**, 5, 2063.
- [18] M. D. Ho, N. Kim, D. Kim, S. M. Cho, H. Chae, *Small* **2014**, 10, 4142.
- [19] D. Dupont, M. D. Tessier, P. F. Smet, Z. Hens, *Adv. Mater.* **2017**, 29, 1700686.
- [20] S. N. Raja, Y. Bekenstein, M. A. Koc, S. Fischer, D. Zhang, L. Lin, R. O. Ritchie, P. Yang, A. P. Alivisatos, *ACS Appl. Mater. Interfaces* **2016**, 8, 35523.
- [21] a) L. Leibler, *Macromolecules* **1980**, 13, 1602; b) F. S. Bates, *Science* **1991**, 251, 898.
- [22] K. Mortensen, E. Theunissen, R. Kleppinger, K. Almdal, H. Reynaers, *Macromolecules* **2002**, 35, 7773.
- [23] a) H. Inagaki, T. Miyamoto, *Die Makromol. Chemie* **1965**, 87, 166; b) L. Wang, P. D. Topham, O. O. Mykhaylyk, H. Yu, A. J. Ryan, J. P. A. Fairclough, W. Bras, *Macromol. Rapid Commun.* **2015**, 36, 1437.
- [24] R. Vehring, *Pharm. Res.* **2008**, 25, 999.
- [25] S. L. Shenoy, W. D. Bates, H. L. Frisch, G. E. Wnek, *Polymer* **2005**, 46, 3372.
- [26] P. Gupta, C. Elkins, T. E. Long, G. L. Wilkes, *Polymer* **2005**, 46, 4799.
- [27] a) Y. Wang, L. Chen, *Macromol. Mater. Eng.* **2012**, 297, 902; b) S. L. Shenoy, W. D. Bates, G. Wnek, *Polymer* **2005**, 46, 8990.
- [28] a) N. Mischenko, K. Reynders, K. Mortensen, R. Scherrenberg, F. Fontaine, R. Graulus, H. Reynaers, *Macromolecules* **1994**, 27, 2345; b) N. K. Dutta, S. Thompson, N. Roy Choudhury, R. Knott, *Phys. B Condens. Matter* **2006**, 385–386, 773.
- [29] J. H. Laurer, A. Rudy Bukovnik, R. J. Spontak, *Macromolecules* **1996**, 29, 5760.
- [30] C. J. Luo, M. Nangrejo, M. Edirisinghe, *Polymer* **2010**, 51, 1654.
- [31] a) J. E. Mark, *Physical Properties of Polymers Handbook*, Springer, New York, NY, USA, **2006**; b) C. M. Hansen, *Hansen solubility parameters: a user's handbook*, CRC

- Press, Boca Raton, FL, USA, **2007**.
- [32] a) W. W. Graessley, *Polymer* **1980**, *21*, 258; b) W. W. Graessley, *Polymeric liquids and networks : structure and properties*, Garland Science, New York, NY, USA, **2004**.
- [33] J. Zhou, X. Man, Y. Jiang, M. Doi, *Adv. Mater.* **2017**, *29*, 1703769.
- [34] a) K. Ozawa, T. Okuzono, M. Doi, *Jpn. J. Appl. Phys.* **2006**, *45*, 8817; b) T. Okuzono, K. Ozawa, M. Doi, *Phys. Rev. Lett.* **2006**, *97*, 136103.
- [35] a) A. Bohr, J. Boetker, T. Rades, J. Rantanen, M. Yang, *Curr. Pharm. Des.* **2014**, *20*, 325; b) J. J. Spillman, *Aeronaut. J.* **1984**, *88*, 181.
- [36] E. Tekin, P. J. Smith, S. Hoepfener, A. M. J. Van Den Berg, A. S. Susa, A. L. Rogach, J. Feldmann, U. S. Schubert, *Adv. Funct. Mater.* **2007**, *17*, 23.
- [37] S. Abe, J. J. Joos, L. I. D. J. Martin, Z. Hens, P. F. Smet, *Light Sci. Appl.* **2017**, *6*.
- [38] a) M. Cirillo, T. Aubert, R. Gomes, R. Van Deun, P. Emplit, A. Biermann, H. Lange, C. Thomsen, E. Brainis, Z. Hens, *Chem. Mater.* **2014**, *26*, 1154; b) L. Carbone, C. Nobile, M. De Giorgi, F. Della Sala, G. Morello, P. Pompa, M. Hytch, E. Snoeck, A. Fiore, I. R. Franchini, M. Nadasan, A. F. Silvestre, L. Chiodo, S. Kudera, R. Cingolani, R. Krahne, L. Manna, *Nano Lett.* **2007**, *7*, 2942; c) E. Drijvers, J. De Roo, P. Geiregat, K. Fehér, Z. Hens, T. Aubert, *Chem. Mater.* **2016**, *28*, 7311.
- [39] B. De Geyter, Z. Hens, *Appl. Phys. Lett.* **2010**, *97*.
- [40] J. Jasieniak, L. Smith, J. Van Embden, P. Mulvaney, M. Califano, *J. Phys. Chem. C* **2009**, *113*, 19468.
- [41] S. Leyre, E. Coutino-Gonzalez, J. J. Joos, J. Ryckaert, Y. Meuret, D. Poelman, P. F. Smet, G. Durinck, J. Hofkens, G. Deconinck, P. Hanselaer, *Rev. Sci. Instrum.* **2014**, *85*.

Figure 1. Schematic representation of the electrospinning process

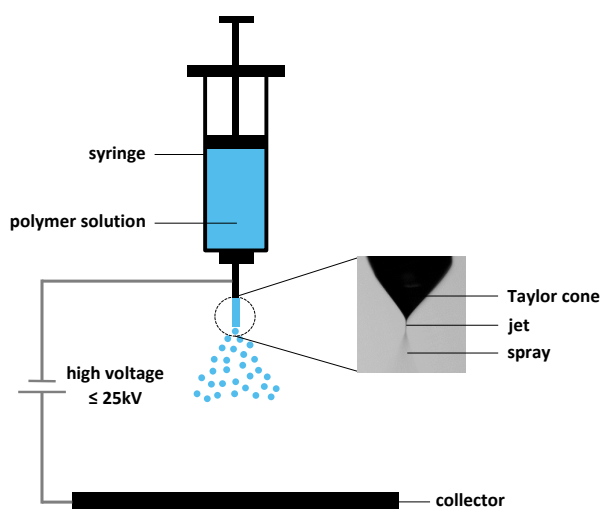


Figure 2. Schematic representation of the microphase structure of SEBS in different solvents. a) structure of SEBS in selective solvent for PS, b) structure of SEBS in selective solvent for PEB and c) chemical formula of SEBS (red = PEB, yellow = PS)

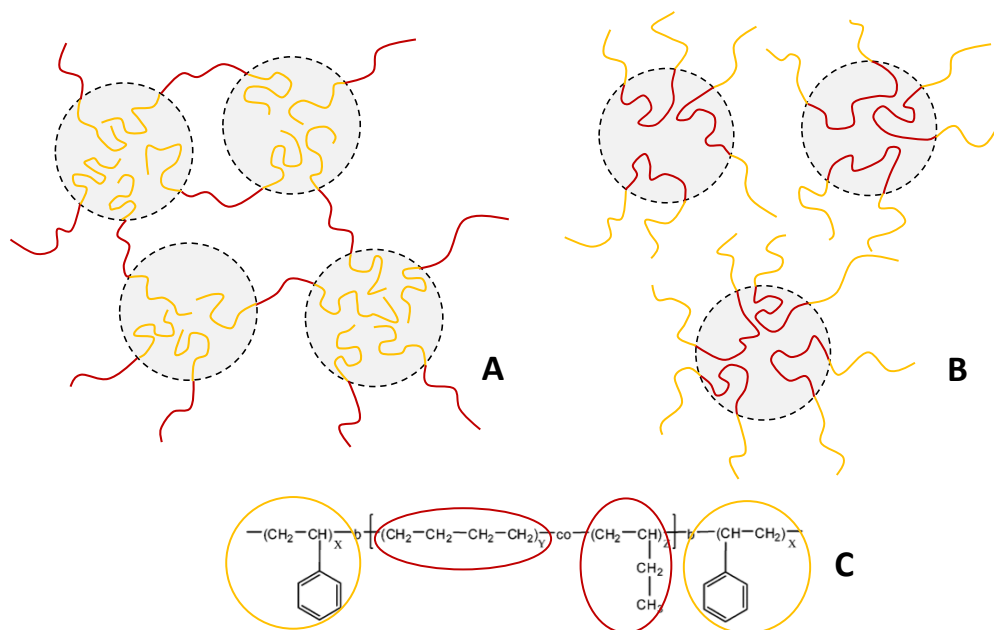


Figure 3. Specific viscosity η_{sp} plotted as a function of concentration to determine the different concentration regimes for SEBS in CHCl_3 .

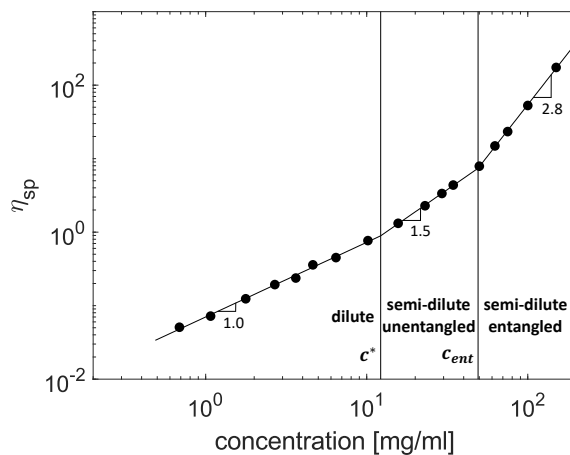


Figure 4. The reduced viscosity η_{red} as a function of concentration for SEBS in CHCl_3 (●) and DCM (■), where the y-axis intercept of the linear fit determines the intrinsic viscosity $[\eta]$.

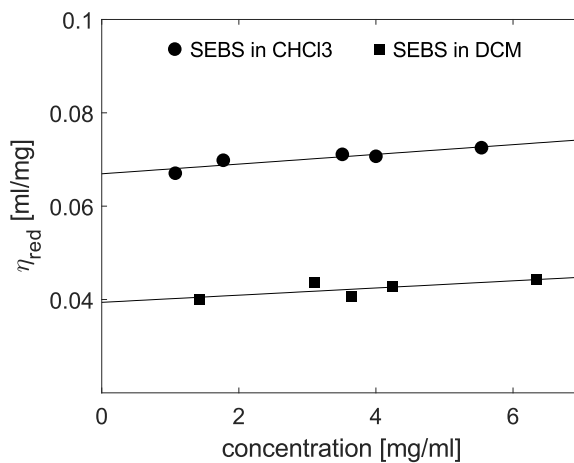


Figure 5. SEM images of electrospayed SEBS in non-selective solvent systems a) CHCl_3 , b) DCM and a schematic representation of the proposed mechanism for the production of the flat particles in c). SEM images of electrospayed SEBS in endblock selective solvent systems d) CHCl_3/DMF 65/35, e) DCM/DMF 80/20 and a schematic representation of the proposed mechanism for the production of the spherical and dense particles in f).

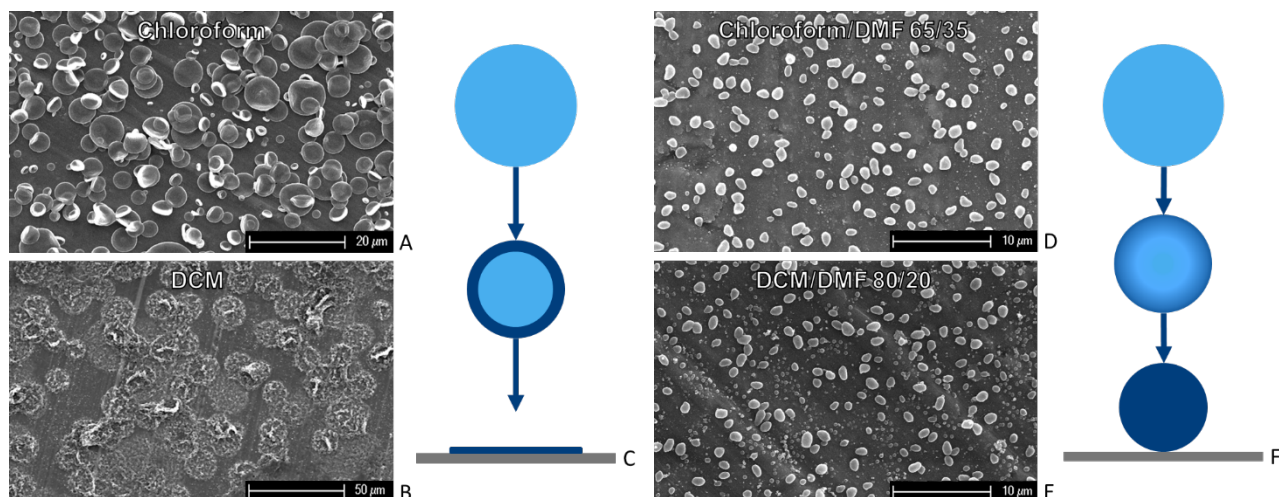


Figure 6. Absorbance (full black line) and emission spectrum (full blue line) of the core/shell CdSe/CdS QDs in CHCl_3 and the absorbance spectrum of pure SEBS (dashed black line)

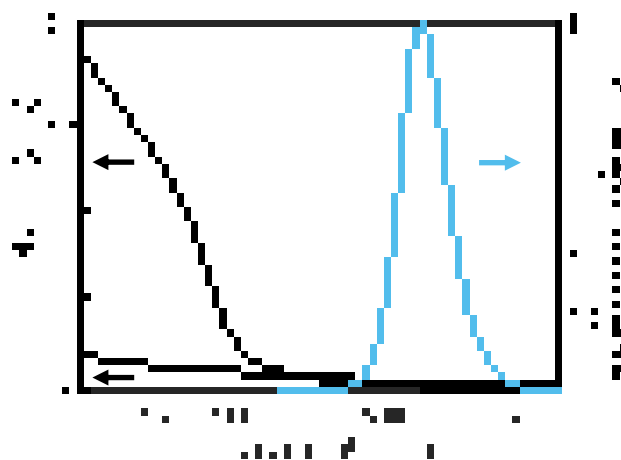


Figure 7. Comparison of the normalized emission spectra for the pure QDs in CHCl_3 and the embedded QDs in SEBS

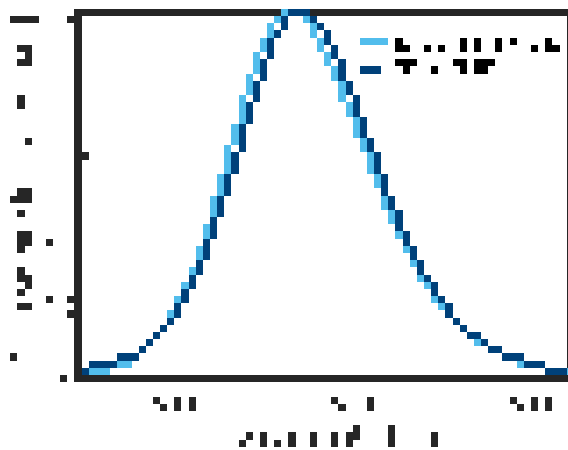


Figure 8. Photodegradation stress tests for the QDs in CHCl_3 and the QD embedded SEBS particles

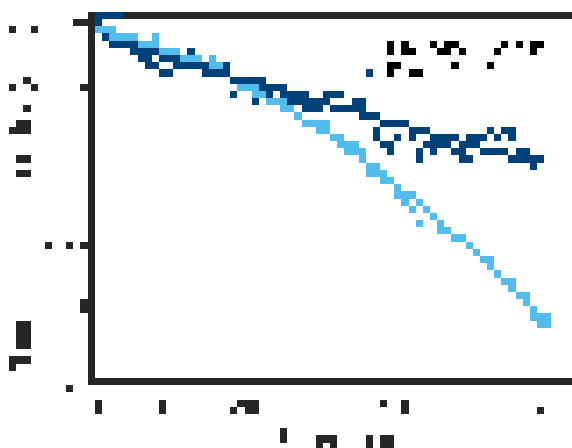


Figure 9. TEM images of the core-shell CdSe/CdS QDs produced according to the described synthesis method, revealing a diameter of 8.1 nm (\pm 1.1 nm)

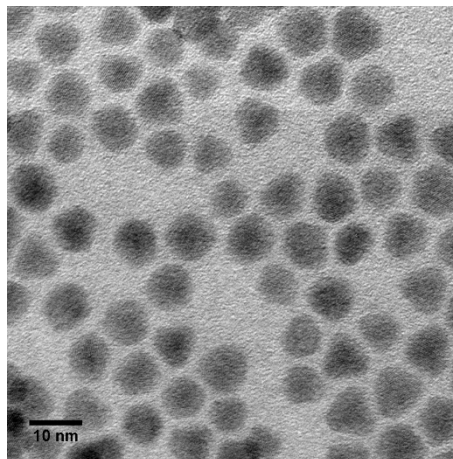


Table 1. GPC results for triblock copolymer SEBS used for the production of polymer particles by electrospaying

M_n [kg/mol]	M_w [kg/mol]	M_z [kg/mol]	PDI
74	81	87	1.09

Table 2. Hansen solubility parameters of the blocks in the triblock copolymer SEBS and solvents of interest.^[31] The relative energy difference RED is calculated as $RED = R_a/R_0$ where the solubility parameter distance between solvent (S) and homopolymer (P) R_a is

determined as $R_a = \sqrt{4(\delta_{D,S} - \delta_{D,P})^2 + (\delta_{P,S} - \delta_{P,P})^2 + (\delta_{H,S} - \delta_{H,P})^2}$ and the interaction sphere radius $R_0 = 8 \text{ MPa}^{1/2}$ for both homopolymers

Homopolymer or solvent	Solubility parameters [$\text{MPa}^{1/2}$]			RED	
	δ_D	δ_P	δ_H	PS	PEB
PS	18.5	4.5	2.9	/	/
PEB	16.9	0.8	2.8	/	/
CHCl3	17.8	4.5	2.9	0.18	0.51
DCM	18.2	6.3	6.1	0.47	0.87
DMF	17.4	13.7	11.3	1.0	1.9
CHCl3/DMF (65/35 v/v)	17.7	7.7	5.8	0.58	1.0
DCM/DMF (80/20 v/v)	18.0	7.78	7.14	0.68	1.0

Embedding of quantum dots (QDs) in polymer particles can improve various undesirable properties like poor biocompatibility and cytotoxicity for *in vivo* and *in vitro* applications. Electro spraying of SEBS proves to be an excellent technique to achieve well dispersed QD encoded polymer particles with a tunable particle morphology from dense spherical to uniformly flat depending on the utilized solvent system.

Keyword Block Copolymers, Colloids, Polymeric Materials, Quantum Dots, Electro spraying

R. Koekoekx, N. C. Zawacka, G. Van den Mooter, Z. Hens, C. Clasen*

Electro spraying the triblock copolymer SEBS: the effect of solvent system and the embedding of quantum dots

